

JOHANNES KAMP¹, STEPHANIE NACHTIGALL², SEBASTIAN MAAß³, MATTHIAS KRAUME⁴

MODELLING OF COALESCENCE IN TURBULENT LIQUID/LIQUID DISPERSIONS CONSIDERING DROPLET CHARGE

Abstract

Drop size distributions in liquid/liquid systems within a turbulent flow, being an integral part of many technical applications, can be simulated solving population balance equations. Experimental investigations in stirred toluene/water systems at constant ionic strength of 0.1 mol/L showed that with pH values higher than 11, coalescence is hindered considerably due to electrostatic effects. Within this work, two designated models are used to simulate the transient drop size distributions in a stirred tank, showing that the influence of droplet charge due to a change in pH value or ion concentration cannot be predicted satisfactorily by existing models. This finding motivates a new modelling approach implementing the DLVO theory into the population balance framework.

Keywords: population balance equation, coalescence, electrostatic force, droplet charge

¹ Dipl.-Ing. Johannes Kamp, Chair of Chemical and Process Engineering, TU Berlin

² Dipl.-Ing. Stephanie Nachtigall, Chair of Chemical and Process Engineering, TU Berlin

³ Dr.-Ing. Sebastian Maaß, Chair of Chemical and Process Engineering, TU Berlin

⁴ Prof. Dr.-Ing. Matthias Kraume, Chair of Chemical and Process Engineering, TU Berlin

1. INTRODUCTION

Dispersions of two immiscible fluids in a turbulent flow are part of many technical processes, like i.e. the liquid/liquid (l/l) extraction or suspension polymerization, and therefore of great interest for the industry. Although, these processes are used frequently, they are by no means completely understood. Thus, the modelling and dimensioning of these are causing serious difficulties. A significant part of the efficiency of these processes is based on the drop size distribution (DSD) within the devices, which is the result of the competing dynamic phenomena of drop breakage and coalescence. A widely used modelling approach of solving population balance equations (PBE) has been used to predict DSD for several applications [1]. Up to now, a reliable prediction of the DSD, depending on chemical, geometrical and process parameters, fails. Existing models include influencing factors of the chemical composition like density, viscosity and interfacial tension, but also electrostatic interactions and mass transfer influence the DSD significantly.

A short overview of existing experimental investigations of DSD in technical devices and an introduction into population balances will be given. Furthermore, existing models in literature will be used to describe the coalescence inhibition at high pH values observed in experiments. Due to insufficient prediction of these models the need for a new modelling approach will be illustrated.

2. STATE OF THE ART

2.1. EXPERIMENTAL INVESTIGATIONS

Due to the major importance of DSD for the technical application of l/l systems, a lot of experimental research has been accomplished until now. For example, the investigations for different devices like extraction columns [2], mixer settler [3], separators [4] and stirred tanks [5] should be mentioned here. Major interest has been the influence of parameters like phase fraction, energy dissipation rate, density, viscosity and interfacial tension.

The coalescence of drops can be influenced massively by the addition of surfactants or electrochemical effects [6, 7] and might even lead to a complete inhibition of coalescence. Electrochemical effects result from a surface charge of a drop induced by i.e. raising the pH value of the system. The surface charge again is dampened by the presence of ions in the continuous phase [8, 9]. In total a repulsing electrostatic force results between two approaching drops. Additionally, in the close-up range of two droplets, the attractive van der Waals force comes into account. The interaction between repulsing electrostatic and attractive van der Waals force is commonly known as DLVO theory, developed independently from each other by Derjaguin and Landau [10] and Verwey and Overbeek [11]. Investigations of Tobin and Ramkrishna [12] show the influence of the drop surface charge in l/l systems. Due to the inhibition of coalescence, the raise of pH value leads to smaller drops in the stirred tank. In contrast, with addition of sodium chloride the coalescence inhibition was reduced, resulting in an increase of the drop size. The decrease of drop size in a stirred tank at pH values higher than 11 has also been described by Gäbler

et al. [5] and Kraume et al. [13] and was also explained by the inhibition of coalescence. Furthermore, Kraume et al. [13] investigated the dependency of coalescence inhibition by NaCl-concentration in shaken flask experiments. It was shown that the settling time, hence the time in which a disperse system separates into two clear phases, tends to decrease with raising salt concentration.

Within this work the considered models will be used to simulate the experimental results from Wegener [14] (shown partially in [5]). The sauter mean diameter has been observed by Wegener at constant ionic strength ($I = 0.1$ mol/L) leading to a sharp decrease of about 40% at pH 13 in comparison to other pH values.

2.2. POPULATION BALANCE EQUATION

The population balance equation, a partial differential equation, describes the time dependent density function $f(d_p, t)$ of particles within a defined volume of the continuous phase. In a batch reactor containing a l/l system, the PBE can be expressed considering only the size change of the particles (in this case drops):

$$\frac{\partial f(d_p, t)}{\partial t} = \dot{B}_b - \dot{D}_b + \dot{B}_c - \dot{D}_c$$

where \dot{B}_i and \dot{D}_i are the death and birth terms of breakage and coalescence, respectively. Each of these terms is expressed by submodels, describing the particular phenomena in detail. For drop breakage the terms can be written as:

$$\dot{B}_b - \dot{D}_b = \int_{d_p}^{\infty} v(d'_p) \cdot \beta(d_p, d'_p) \cdot g(d'_p) \cdot f(d'_p, t) dd'_p - g(d_p) \cdot f(d_p, t)$$

containing the drop breakage rate $g(d_p)$, the daughter drop size distribution $\beta(d_p, d'_p)$ and the number of daughter droplets created by drop breakup $v(d_p)$.

The terms of coalescence are developed using the definition $d_p'' = (d_p^3 - d_p'^3)^{1/3}$:

$$\dot{B}_c - \dot{D}_c = \frac{1}{2} \int_0^{d_p} F(d_p'', d'_p) \cdot f(d'_p, t) \cdot f(d_p'', t) dd'_p - f(d_p, t) \cdot \int_0^{\infty} F(d_p, d'_p) \cdot f(d'_p, t) dd'_p$$

with the coalescence rate $F(d_p, d'_p)$. A detailed discussion of PBE in general can be found in Ramkrishna [1] and Liao and Lucas [15, 16] who reviewed breakage and coalescence models for l/l systems.

For all simulations showed here a Gaussian daughter drop size distribution $\beta(d_p, d'_p)$ and binary drop breakup ($v(d_p) = 2$) is assumed. In this work the commonly used model for l/l systems from Coualoglou and Tavlarides [17] will be compared with the only model in literature including electrostatic effects from Tobin and Ramkrishna [18]. These two models will be presented shortly, for detailed information see corresponding literature.

2.2.1. MODEL OF COULALOGLOU & TAVLARIDES

Coualoglou and Tavlarides [17] proposed a phenomenological model for l/l systems using PBE, in which the breakage rate $g(d_p)$ is assumed to be a product of the fraction of breaking drops and the reciprocal time needed for the drop breakup to occur, which results in the following:

$$g(d_p) = c_{1,b} \frac{\varepsilon^{1/3}}{(1+\varphi)d_p^{2/3}} \exp\left(-c_{2,b} \frac{\gamma(1+\varphi)^2}{\rho_d \varepsilon^{2/3} d_p^{5/3}}\right).$$

The factor $(1+\varphi)^{-1}$ was introduced subsequently by Coualaloglou and Tavlarides [17] to account for the damping effect of droplets on local turbulent intensities.

The coalescence rate $F(d_p, d'_p)$ is defined as the product of the collision frequency $\xi(d_p, d'_p)$ and the coalescence efficiency $\lambda(d_p, d'_p)$:

$$F(d_p, d'_p) = \xi(d_p, d'_p) \cdot \lambda(d_p, d'_p).$$

The collision frequency expresses how often drops in the system collide and interact with each other. Assuming an analogy between collisions of drops in a locally isotropic flow field and collisions of molecules as in the kinetic theory of gases, yields

$$\xi(d_p, d'_p) = c_{1,c} \frac{\varepsilon^{1/3}}{1+\varphi} (d_p + d'_p)^2 (d_p^{2/3} + d'^{2/3}_p)^{1/2}. \quad 5$$

This collision frequency is a modified version of the original one, published by Tsouris and Tavlarides [19].

The coalescence efficiency corresponds to the probability that two collided drops coalesce. Having a closer look at the collision of drops, the coalescence efficiency is described by relating the contact time of two drops to the time required for the drainage of the thin film of continuous phase between these drops:

$$\lambda_{c\&t}(d_p, d'_p) = \exp\left(-c_{2,c} \frac{\eta_c \rho_c \varepsilon}{\gamma^2 (1+\varphi)^3} \left(\frac{d_p \cdot d'_p}{d_p + d'_p}\right)^4\right).$$

With this work Coualaloglou and Tavlarides achieved a mechanistic model for I/I systems which is still frequently used nowadays. To fit experimental data, the model contains four numerical parameters.

2.2.2. MODEL OF TOBIN & RAMKRISHNA

The PBE model proposed by Tobin and Ramkrishna [18] was motivated by earlier investigations in a stirred tank by the same authors in which an influence of ionic strength and pH on the coalescence rate was observed [12]. It is the only model known to the author taking electrostatic interactions into account. As the investigators only study the droplet coalescence rate in a stirred tank by reducing the impeller frequency abruptly, the developed model does not include breakage terms in the PBE. The overall coalescence efficiency is calculated from the product of the coalescence efficiency of a rigid and a deformable drop:

⁵ Corrected erratum: power of 1/2 instead of 1/3

$$\lambda_{T\&R}(d_p, d'_p) = \lambda_{\text{rigid}}(d_p, d'_p) \cdot \lambda_{\text{deformable}}(d_p, d'_p)$$

$$= \frac{1 - \exp\left[\frac{-c_{2,c} Z_1 \eta_c}{\rho_c \bar{d}^{2/3} \varepsilon^{1/3}} \left(1 - \frac{c_0}{\rho_c \bar{d}^{2/3} \varepsilon^{1/3}}\right)\right]}{1 - \exp\left[\frac{-c_{2,c} Z_2 \eta_c}{\rho_c \bar{d}^{2/3} \varepsilon^{1/3}} \left(1 - \frac{c_0}{\rho_c \bar{d}^{2/3} \varepsilon^{1/3}}\right)\right]} \cdot \frac{1 - \exp\left[\frac{-c_{2,c} Z'_1 \eta_c \rho_c \varepsilon \bar{d}^4}{(2\gamma h_s)^2} \left(1 - \frac{c_1 \bar{d}}{2\gamma}\right)\right]}{1 - \exp\left[\frac{-c_{2,c} Z'_2 \eta_c \rho_c \varepsilon \bar{d}^4}{(2\gamma h_s)^2} \left(1 - \frac{c_1 \bar{d}}{2\gamma}\right)\right]}$$

using the mean drop diameter $\bar{d} = (d_p \cdot d'_p) / (d_p + d'_p)$.

The parameters Z_i and Z'_i depend on the dimensionless film thicknesses H_1 (describing the distance of two drops at which film separation begins) and H_2 (representing the characteristic film thickness at which film rupture occurs) formed with the distance h_s at which the two drops are no longer considered to be in contact with each other:

$$H_i = \frac{h_i}{h_s} \quad Z_i = -\log(H_i) \quad Z'_i = \frac{1 - H_i^2}{2H_i^2}.$$

Corresponding to the implementation in the original paper, these parameters are set to $h_s = 1000$ nm, $h_1 = 500$ nm and $h_2 = 50$ nm as well as setting the two parameters c_0 and c_1 equal to one another: $c_{3,c} = c_0 = c_1$. This lumped numerical parameter $c_{3,c}$ is introduced by the authors to describe the influence of the electrostatic repulsion force. However, the dependency of this parameter on system parameters, like pH and ionic strength, is unknown and has to be fitted for each system composition individually.

With this work Tobin and Ramkrishna presented an approach to consider electrostatic repulsion forces using one additional numerical parameter. Varying the characteristic distances H_1 and H_2 would even increase the number of fitting parameters additionally.

3. MATERIALS AND METHODS

All experiments have been carried out using deionised water as continuous phase and toluene (Merck 1.08325.2500 p.a.) as disperse phase. To set the pH value and ionic strength sodium respectively potassium hydroxide (Merck 1.09956.0001 / 1.09921.0001 p.a.), hydrochloric acid (Merck 1.09970.001 p.a.) and sodium respectively potassium chloride (Merck 1.06404.0500 / 1.04936.0500 p.a.) were used. All equipment used (except the flow channel of single drop experiments) is made of glas, stainless steel or PTFE to avoid contaminations. Furthermore, all equipment was rinsed with deionised water extensively prior to use.

Single drop breakage investigations were performed in a rectangular channel in which a single blade representative of a section of a Rushton turbine is fixed. Toluene drops flowing with the continuous phase through the channel interact with the impeller blade and were recorded by a high speed camera. A detailed description of this set-up is given in [20]. In order to increase the optical properties of the image data, the toluene was blended with a non-water soluble dye ($c_{\text{dye}} = 0.075$ g/L). Two droplet diameters ($d_p = 0.66$ mm and $d_p = 2.0$ mm) were investigated. KOH was added to the water phase to set pH 13. Additionally, for all set-ups, KCl was added in a concentration of $c_{\text{KCl}} = 0.16$ g/L to ensure

the proper work of the fluid flow meter. The fluid flow velocity of the continuous water phase was kept constant ($v = 1.5$ m/s at the stirrer blade). The number of breaking drops was set into relation to the total number of investigated droplet sequences (at least 1000), to calculate the breakage probability.

Investigations in a stirred tank DN 150⁶ were performed using an endoscope technique to detect the drop size distribution. Continuous phase was water with added NaOH, NaCl and HCl to set pH and a constant ionic strength ($I = 0.1$ mol/L) [14]. For detailed description of this set-up and measurement technique see [21].

The interfacial tension was measured using sodium and potassium chloride and their corresponding acid and base, respectively. Two methods have been used to determine the interfacial tension. The first one was the pendant drop method [22] carried out on a Data Physics OCA 20. This is probably the most convenient, versatile and popular method to measure the surface tension. Here the geometry of a drop is analyzed optically and the profile is related to the surface tension through a nonlinear differential equation [23]. Additionally, the interfacial tension was measured with a KRÜSS surface tensiometer Model K10 using the ring method. The standard procedure was used, following the works of Cupples [24]. Opposed to the pendant drop method, the ring method only provides values for the steady state of the interfacial tension. However, both methods were in good agreement for the steady state values.

To solve the PBE the commercial software PARSIVAL [25] is used. The experimental stirrer frequencies ($n = 400, 550, 700$ min⁻¹) correspond to a mean energy dissipation rate in the tank of $\varepsilon = 0.133, 0.345$ and 0.712 m²/s³. To account for the locally increased energy dissipation near the impeller, the mean dissipation rates were multiplied with the factor $f_\varepsilon = 7.26$ [19]. The numerical parameters of the coalescence rate were fitted to experimental data. The applied procedure was to fit the ‘hydrodynamic’ parameters $c_{1,c}$ and $c_{2,c}$ to experimental data at pH 7 and $n = 550$ min⁻¹. Afterwards, the ‘electrostatic’ parameter $c_{3,c}$ was adapted to experimental data at pH 13 when necessary.

4. RESULTS

In the following the possibilities of simulating the DSD in a stirred tank together with the observed coalescence inhibition due to raising pH will be discussed. To avoid a misinterpretation of the influence of electrostatic effects on drop coalescence, the impact of pH on interfacial tension and drop breakage is determined. Afterwards, the models of Coulaloglou and Tavlarides and Tobin and Ramkrishna will be used to simulate the experimental results.

The influence of ionic strength on the interfacial tension was investigated from $I = 0$ to 0.1 mol/L. No significant effect exceeding the measurement error could be observed (data not shown), thus influence of ionic strength on the interfacial tension can be neglected. Measurements varying the pH value (see fig. 1) show a constant value of $\gamma = 35 \pm 1$ mN/m for pH 1 to 11, which is comparable to the literature value ($\gamma = 36.1$ mN/m)

⁶ Corrected erratum: DN 150 instead of DN 100

of Misek [26] measured at pH 7 with no additional electrolytes. At pH 13 a significant decrease of interfacial tension was observed. To account for this influence, all simulations at pH 13 were done using $\gamma = 32 \text{ mN/m}$, which results in a decrease of the sauter mean diameter about 10% [27]. Thus, interfacial tension is not the sole reason for the decrease of sauter mean diameter at high pH values.

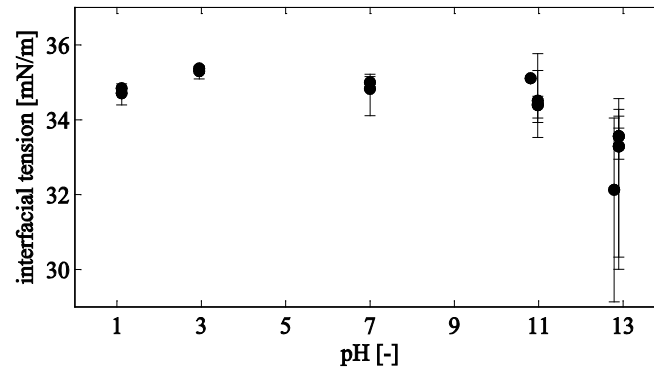


Fig. 1. Interfacial tension of system toluene/water for various pH values

Investigations of single drops breaking near an impeller were conducted to eliminate the possibility of electrostatic effects having an additional effect on the drop breakage. In table 1 the breakage probabilities at pH 7 from [20] and measurements at pH 13 are shown. As the breakage rates are nearly constant when varying the pH value, droplet breakage can be assumed to be independent from electrostatic effects.

Table 1

Breakage probabilities for different droplet diameters and pH values

droplet diameter d_p	pH 7 from [20]	pH 13
[mm]	[-]	[-]
0.66	45 %	44 %
2.00	75 %	73 %

4.1. SIMULATIONS USING COULALOGLOU & TAVLARIDES MODEL

Simulations of a stirred tank using the Coualaloglou and Tavlarides model were performed with the original numerical parameters for the breakage rate [17]. To fit the experimental data, numerical parameters of the coalescence rate were adapted to the experimental data at pH 7 and $n = 550 \text{ min}^{-1}$ (see table 2). As the model does not account for electrostatic interactions and all parameters (including interfacial tension) are constant, the simulations yield identical results for pH values 1 to 11. In order to predict the experimental values at

pH 13, the numerical parameter $c_{2,c}$ of the coalescence probability was changed. The result of these two parameter sets can be seen in fig. 2. On the left hand side, transient simulations at a stirrer frequency of $n = 550 \text{ min}^{-1}$ with the two parameter sets are shown at pH 7 and 13 respectively. There are deviations between first experimental value and simulation noticeable, but the stationary state of the sauter mean diameter is well predicted by the model. On the right hand side, the stationary values of experiments and simulations are plotted against pH value at the three stirrer frequencies. As mentioned above, the simulation result is constant for pH 1–11 for each stirrer frequency. The adapted parameter set has been used to simulate at pH 13, interpolating linearly from pH 11. For the stirrer frequencies $n = 550 \text{ min}^{-1}$ and 700 min^{-1} the simulations describe the experimental data quite good. However, at the stirrer frequency of $n = 400 \text{ min}^{-1}$ a significant aberration can still be observed.

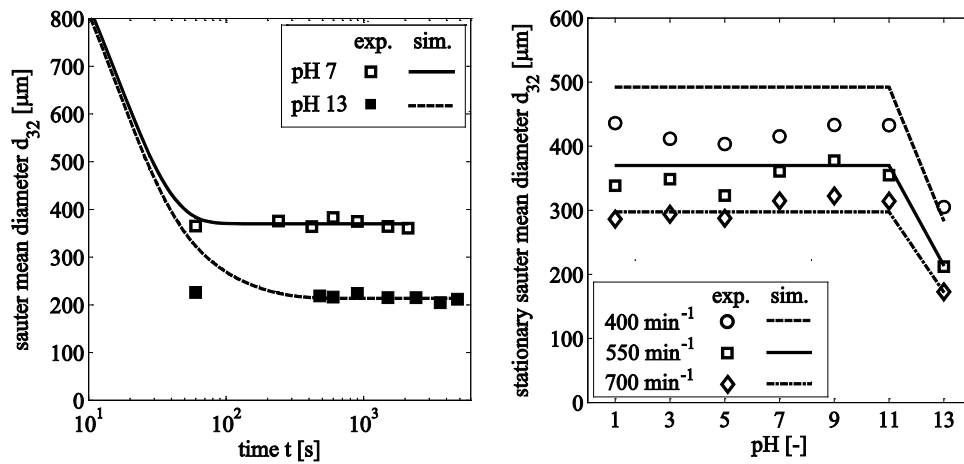


Fig. 2. Sauter mean diameter d_{32} vs. time at $n = 550 \text{ min}^{-1}$ (left) and stationary d_{32} vs. pH (right) simulated with model of Coualoglou and Tavlarides [17]

Table 2

Numerical parameters of PBE models used

Model	$C_{1,b}$	$C_{2,b}$	$C_{1,c}$	$C_{2,c}$	$C_{3,c}$
Coualoglou & Tavlarides pH 7	$2.5151 \cdot 10^{-3}$	$2.0696 \cdot 10^{-1}$	$1.75 \cdot 10^{-3}$	$1.6257 \cdot 10^{12}$	-
Coualoglou & Tavlarides pH 13	$2.5151 \cdot 10^{-3}$	$2.0696 \cdot 10^{-1}$	$1.75 \cdot 10^{-3}$	$3.1257 \cdot 10^{13}$	-
Tobin & Ramkrishna pH 7	$2.5151 \cdot 10^{-3}$	$2.0696 \cdot 10^{-1}$	$1.75 \cdot 10^{-3}$	$8.45 \cdot 10^{-1}$	$1.0 \cdot 10^{-6}$
Tobin & Ramkrishna pH 13	$2.5151 \cdot 10^{-3}$	$2.0696 \cdot 10^{-1}$	$1.75 \cdot 10^{-3}$	$8.45 \cdot 10^{-1}$	$2.25 \cdot 10^{-3}$

4.2. SIMULATIONS USING TOBIN & RAMKRISHNA MODEL

Due to the fact that the PBE model of Tobin and Ramkrishna does not consider any breakage kernel, it is not suitable for simulations of systems in which breakage events

occur. In the experiments discussed [14] the dispersion of toluene in a stirred tank starting with two separate phases was investigated and therefore the implementation of a breakage kernel is inevitable. For this purpose the breakage kernel of Coualaloglou and Tavlarides was used, as well as their collision frequency. Thus, the difference to the previous simulations is the implementation of the coalescence efficiency. Accordingly to the mentioned procedure of fitting the numerical parameters, firstly the coalescence parameters $c_{1,c}$ and $c_{2,c}$ were adapted to the experimental data at pH 7 and $n = 550 \text{ min}^{-1}$, setting the parameter $c_{3,c} = 1.0 \cdot 10^{-6}$ which corresponds to negligible electrostatic effects (see table 3.2). The breakage parameters remained untouched. Subsequently, the electrostatic parameter $c_{3,c}$ was fitted to the experimental data at pH 13 and $n = 550 \text{ min}^{-1}$. The corresponding simulations can be seen in fig. 3. In analogy to fig. 2, on the left hand side transient simulations at a stirrer frequency of $n = 550 \text{ min}^{-1}$ with the two parameters sets are shown at pH 7 and 13 respectively. In comparison to fig. 2, the experimental stationary sauter mean diameter is reached later with these simulations. In addition, the stationary sauter mean diameter at pH 13 differs significantly from the experimental value. This aberration could not be eliminated by varying only the electrostatic parameter $c_{3,c}$. Fitting parameter $c_{2,c}$ additionally, the steady state of the experimental sauter mean diameter could be predicted but the transient behaviour was still worse compared to the results of Coualaloglou and Tavlarides model (data not shown). On the right hand side, plotting the stationary values of experiments and simulations against pH value at the three stirrer frequencies, it can be seen clearly that the coalescence model of Tobin and Ramkrishna does not depict the influence of the stirrer frequency correctly in this case.

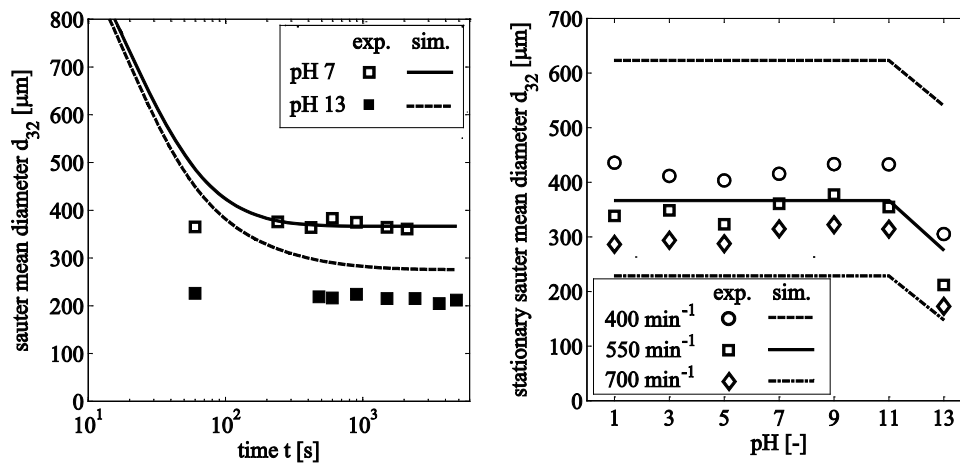


Fig. 3. Sauter mean diameter d_{32} vs. time at $n = 550 \text{ min}^{-1}$ (left) and stationary d_{32} vs. pH (right) simulated with model of Tobin and Ramkrishna [18]

Comparing the two simulation approaches, it can be concluded that the model of Coualaloglou and Tavlarides is able to predict the experimental data better than the one of Tobin and Ramkrishna. This is especially the case considering the dependency of the stirrer frequency and therefore the power input. Since the Coualaloglou and Tavlarides model does

not account for electrostatic effects, it is quite interesting that it performs better than the model of Tobin and Ramkrishna. For both models one numerical parameter has to be varied to describe the coalescence inhibition at high pH values. For this purpose, the model of Tobin and Ramkrishna even needs one extra numerical parameter which has to be fitted additionally for every application. Varying the representative distances h_1 and h_2 may improve simulating results, but also increases the number of adapting parameters by two. Furthermore, it is questionable to define a constant critical distance $h_2 = 50$ nm at which coalescence occurs, knowing that the resulting repulsion force strongly depends on ionic strength [10, 11] and only reaches significant values at a distance of a few (about 2 - 20) nanometers in l/l systems [28]. Varying the factor f_e , which accounts for locally increased energy dissipation, shifts the numerical parameters but does not change the shown characteristics of the models in this single zone modelling approach. This effect can be seen directly in the Coualaloglou and Tavlarides model, but also accounts for the model of Tobin and Ramkrishna (data not shown).

5. SUMMARY AND OUTLOOK

It could be shown that the experimental finding of smaller drop sizes with increasing pH is not only determined by a decrease of interfacial tension but also depends on the electrostatic interaction of droplets. As the electrostatic effect does not influence the drop breakage, as shown in experimental investigations of single drop breakup, it can only result in an inhibition of coalescence. Trying to simulate this coalescence inhibition, it is shown that the standard model of Coualaloglou and Tavlarides is able to describe the experimental data better with varying one coalescence parameter than the model of Tobin and Ramkrishna. Although, the latter accounts for electrostatic repulsion in model development also using one varying parameter.

To include electrostatic effects, i.e. induced by a pH shift within a reactor, the PBE modelling has to be extended by a physically based model with a constant numerical parameter. To maintain the model kit system of PBE, this new model should be combinable with existing models of electrostatic efficiency. A model fulfilling these demands has been developed by the author successfully. For this purpose, the surface charge of droplets have been quantified and implemented into PBE framework using the DLVO theory. This modelling approach will be presented on 19th International Conference Process Engineering and Chemical Plant Design and published forthcoming.

S y m b o l s

\dot{B}_i	– birth rate	[1/s]
$c_{i,b}$ $c_{i,c}$	– numerical parameters for breakage & coalescence	[various]
c	– concentration	[g/L]
d_{32}	– sauter mean diameter	[m]
d_p	– particle diameter	[m]

\bar{d}	– mean particle diameter	[m]
\dot{D}_i	– death rate	[1/s]
ε	– energy dissipation rate	[m ² /s ³]
f_ε	– factor accounting for increase of ε near impeller	[-]
f	– density function	[m ⁻³]
F	– coalescence rate	[m ³ /s]
g	– breakage rate	[s ⁻¹]
γ	– interfacial tension	[N/m]
h_i	– characteristic distances	[m]
H_i	– dimensionless characteristic distances	[-]
I	– ionic strength	[mol/L]
λ	– coalescence efficiency	[-]
n	– stirrer rotational frequency	[min ⁻¹]
η_c	– dynamic viscosity of continuous phase	[Pa s]
φ	– volume fraction	[-]
ζ	– collision frequency	[m ³ /s]
$\rho_c \rho_d$	– density of continuous & disperse phase	[kg/m ³]
t	– time	[s]
v	– velocity	[m/s]
$Z_i c_i$	– parameters in Tobin & Ramkrishna model	[various]

Literature

- [1] Ramkrishna D.: *Population balances*. Academic Press, San Diego 2000
- [2] Gomes L.N., Guimaraes M.L., Lopes J.C., Madureira C.N., Stichlmair J., Cruz – Pinto J.J.: *Reproducibility of the Hydrodynamic Performance and Measurements in a Liquid-Liquid Kühni Extraction Column-Relevance to Theoretical Model Evaluation*. *Industrial & Engineering Chemistry Research*, **43**(4), (2004), 1061-1070, Doi:10.1021/ie030277i
- [3] Davies G.A., Jeffreys G.V., Smith D.V.: *Rate of coalescence of the dispersed phase in a laboratory mixer settler unit. II. Analysis of coalescence in a continuous mixer settler system by a differential model*. *AIChE J.*, **16**, (1970), 827–831
- [4] Frising T., Noik C., Dalmazzone C.: *The liquid-liquid sedimentation process: From droplet coalescence to technologically enhanced water-oil emulsion gravity separators: A review*. *Journal of Dispersion Science and Technology*, **27**, (2006), 1035–1057. Doi:10.1080/01932690600767098
- [5] Gäbler A., Wegener., Paschedag A., Kraume M.: *The effect of pH on experimental and simulation results of transient drop size distributions in stirred liquid-liquid dispersions*. *Chemical Engineering Science*, **61**(9), (2006), 3018-3024
- [6] Rambhaud., Phadke D.S., Dorle A.K.: *Evaluation of o/w emulsion stability through zeta potential. I. J. Soc. Cosmet. Chem*, **28**, (1977), 183–196

- [7] W a t a n a b e A.: *Electrochemistry of oil-water interfaces*, In: M a t i j e v i c, E.: Surface and Colloid Science, **13**, Plenum Press, New York 1984, 1–70
- [8] L y k l e m a J., v a n L e e u w e n H.P., M i n o r M.: *DLVO-theory, a dynamic re-interpretation*. Advances in Colloid and Interface Science, **83**(1-3), (1999), 33–69. Doi:10.1016/S0001-8686(99)00011-1
- [9] L y k l e m a J.: *Fundamentals of Interface and Colloid Science: Liquid-fluid interfaces*, Academic Press, London 2000
- [10] D e r j a g u i n B.V., L a n d a u E.M.: *Theory of the stability of strongly charged lyophobic sols and of the adhesion of strongly charged particles in solutions of electrolytes*. Acta Physicochimica U.R.S.S, **14**, (1941), 633–662
- [11] V e r w e y E.J.W., O v e r b e e k J.T.G.: *Theory of the Stability of Lyophobic Colloids*, Elsevier 1948
- [12] T o b i n T., R a m k r i s h n a D.: *Coalescence of charged droplets in agitated liquid-liquid dispersions*. AIChE Journal, **38**(8), (1992), 1199-1205. Doi:10.1002/aic.690380807
- [13] K r a u m e M., G ä b l e r A., S c h u l z e K.: *Influence of physical properties on drop size distributions of stirred liquid-liquid dispersions*. Chemical Engineering & Technology, **27**(3), (2004), 330–334
- [14] W e g e n e r M.: *Experimentelle Untersuchungen und Modellierung von transienten Tropfengrößenverteilungen in gerührten Flüssig-flüssig-Systemen*, Master thesis, Chair of Chemical and process Engineering, TU Berlin, Germany 2004
- [15] L i a o Y., L u c a s D.: *A literature review of theoretical models for drop and bubble breakup in turbulent dispersions*. Chemical Engineering Science, **64**(15), (2009), 3389–3406. Doi:10.1016/j.ces.2009.04.026
- [16] L i a o Y., L u c a s D.: *A literature review on mechanisms and models for the coalescence process of fluid particles*. Chemical Engineering Science, **65**, (2010), 2851–2864. Doi:10.1016/j.ces.2010.02.020
- [17] C o u l a l o g l o u C.A., T a v l a r i d e s L.L.: *Description of interaction processes in agitated liquid-liquid dispersions*. Chemical Engineering Science, **32**, (1977), 1289–1297. Doi:10.1016/0009-2509(77)85023-9
- [18] T o b i n T., R a m k r i s h n a D.: *Modeling the effect of drop charge on coalescence in turbulent liquid-liquid dispersions*. The Canadian Journal of Chemical Engineering, **77**(6), (1999), 1090-1104. Doi:10.1002/cjce.5450770603
- [19] T s o u r i s C., T a v l a r i d e s L. L.: *Breakage and Coalescence Models for Drops in Turbulent Dispersions*. AIChE Journal, **40**(3), (1994), 395–406
- [20] M a a ß S., K r a u m e M.: *Determination of breakage rates using single drop experiments*. Chemical Engineering Science, **70**, (2012), 146–164. Doi:10.1016/j.ces.2011.08.027
- [21] M a a ß S., W o l l n y S., V o i g t A., K r a u m e M.: *Experimental comparison of measurement techniques for drop size distributions in liquid/liquid dispersions*. Experiments in Fluids, **50**(2), (2011), 259–269. Doi:10.1007/s00348-010-0918-9
- [22] J o n D.I., R o s a n o H.L., C u m m i n s H.Z.: *Toluene Water/1-Propanol Interfacial-Tension Measurements by Means of Pendant Drop, Spinning Drop, and Laser Light-Scattering Methods*. J. Colloid Interface Science, **114**, (1986), 330–341

- [23] Arashiro E.Y., Demarquette N.R.: *Use of the Pendant Drop Method to Measure Interfacial Tension between Molten Polymers*. *Materials Research*, **2**, (1999), 23–32
- [24] Cupples H.L.: *Interfacial Tension by the Ring Method - the Benzene-Water Interface*. *Journal of Physical and Colloid Chemistry*, **51**, (1947), 1341–1345
- [25] Wulkow M., Gerstlauer A., Nieken U.: *Modeling and simulation of crystallization processes using parsival*. *Chemical Engineering Science*, **56**(7), (2001), 2575–2588. Doi:10.1016/S0009-2509(00)00432-2
- [26] Misek T., Berger R., Schröter J.: *Standard Test Systems for Liquid Extraction*, 2nd edn. EFCE Publication Series 46, European Federation of Chemical Engineering, Warwickshire 1985
- [27] Maaß S., Paschedag A.R., Kraume M.: *Influence of Electrolytes and Turbulence Parameters on Drop Breakage and Drop Size Distributions in Stirred Liquid/Liquid Dispersions*. In: *Proceedings of 6th International Conference on Multiphase Flow*, Leipzig 2007
- [28] Pfennig A., Schwerin A.: *Influence of Electrolytes on Liquid-Liquid Extraction*. *Industrial & Engineering Chemistry Research*, **37**(8), (1998), 3180–3188. Doi:10.1021/ie970866m